

## Composition and structure of nitrogen-containing dispersoids in trimodal aluminum metal–matrix composites

C. Hofmeister · B. Yao · Y. H. Sohn · T. Delahanty ·  
M. van den Bergh · K. Cho

Received: 10 February 2010/Accepted: 27 April 2010/Published online: 14 May 2010  
© Springer Science+Business Media, LLC 2010

**Abstract** Trimodal aluminum (Al) metal–matrix-composites (MMCs), consisting of B<sub>4</sub>C particulates, a nanocrystalline Al (NC-Al) phase, and a coarse-grain Al phase (CG-Al), has been fabricated. These MMCs exhibits extremely high compressive strength and tailorable ductility. Excellent thermal stability of NC-Al grains and high strength has been attributed partially to the nitrogen present within the trimodal Al MMCs, which is introduced during the cryomilling process in liquid nitrogen. This paper describes an investigation into the concentration and constituents of nitrogen within the trimodal Al MMCs. The structure of nitrogen-containing dispersoids was examined by analytical transmission electron microscopy (TEM), and secondary ion mass spectrometry (SIMS) was employed to determine the total concentration of nitrogen. The nitrogen concentration increased linearly with an increase in cryomilling time up to 24 h. Both crystalline and amorphous aluminum nitrides with very fine size, down to 5 nm, as dispersoids, have been observed by analytical TEM.

Correlations between the cryomilling time, nitrogen concentration, NC-Al grain size, and composite hardness are presented and discussed. The presence of nitrogen as nitride-dispersoids can contribute to the outstanding mechanical properties of trimodal Al MMCs by inhibiting NC-Al grain growth during the high temperature consolidation and deformation process, and by dispersion-strengthening.

### Introduction

Nanostructured aluminum (Al) alloy based metal–matrix-composites (MMCs) have gained considerable interest due to their excellent properties (e.g., high strength, low density, good corrosion resistance, etc.), and good potential for commercial-scale manufacturing [1–3]. However, a low-tensile ductility exhibited at room temperature by these nanocrystalline composites can limit their practical applications [4–6]. Recently, trimodal Al MMCs consisting of a nanocrystalline Al phase (NC-Al), boron carbide (B<sub>4</sub>C) reinforcement particles, and a coarse-grain Al phase (CG-Al) have been successfully fabricated, which exhibits an extremely high compressive yield strength and tailorable ductility [7–9]. The fabrication of these composites begins with a cryomilling of inert-gas atomized AA5083 Al alloy powders (i.e., –325 mesh, inert-gas atomized AA5083 Al alloy powders less than 44 µm in size) and B<sub>4</sub>C particles (i.e., 1–5 µm in size). This yields agglomerates of NC-Al grains containing a uniform dispersion of solidly bonded, sub-micron B<sub>4</sub>C particles. The B<sub>4</sub>C/NC-Al agglomerates are then size classified, and blended with CG-Al powders. The blended powders are then vacuum degassed, and consolidated by conventional powder metallurgy techniques such as vacuum hot pressing (VHP), or

C. Hofmeister · B. Yao · Y. H. Sohn (✉)  
Advanced Materials Processing and Analysis Center and  
Department of Mechanical, Materials and Aerospace  
Engineering, University of Central Florida, Orlando,  
FL 32816, USA  
e-mail: ysohn@mail.ucf.edu

T. Delahanty  
Pittsburgh Materials Technology, Inc., Jefferson Hills,  
PA 15025, USA

M. van den Bergh  
DWA Aluminum Composites, Chatsworth, CA 91311, USA

K. Cho  
U.S. Army Research Laboratory, Aberdeen Proving Ground,  
MD 21005, USA

hot or cold isostatic pressing (HIP or CIP) to form bulk trimodal Al MMCs. The B<sub>4</sub>C particles and NC-Al phase provide the high strength, and the introduction of CG-Al phase improves the ductility of the composite [7–9].

The cryomilling of B<sub>4</sub>C particles and Al alloy powders in liquid nitrogen is a critical, initial step [10, 11] that reduces the grain size of the Al phase, decreases the B<sub>4</sub>C particle size, and forms the solid B<sub>4</sub>C/NC-Al bonding within the agglomerates, while minimizing the oxidation and recrystallization of the NC-Al powders. Another merit of cryomilling is the mechanical alloying of nitrogen into the NC-Al [12–14]. It has been reported that the nitrogen content in the cryomilled-agglomerates can reach up to 1.0 wt% [12, 13]. Many excellent properties exhibited by trimodal Al MMCs, such as high thermal stability of NC-Al grains and high strength, have been attributed partially to the presence of nitrogen [12, 13]. Knowledge of the concentration, distribution, and constituents of nitrogen in trimodal MMCs can provide a better understanding for the efficient optimization of the manufacturing process and the composite properties.

In this study, analytical transmission electron microscopy (TEM) and secondary ion mass spectrometry (SIMS) have been used to examine the overall nitrogen concentration and structure of nitrogen-containing dispersoids in trimodal Al MMC specimens with different processing routes. Several analytical TEM techniques have been utilized to examine the distribution and constituents of nitrogen-containing dispersoids within the composites, including electron energy loss spectrometry (EELS), high-resolution TEM (HRTEM), and hollow-cone dark field (HCDF). It has been found that nitrogen is non-uniformly present within the composites. Both crystalline and amorphous aluminum nitrides have been observed within the NC-Al grains, NC-Al grain boundaries, and at the interfaces between the NC-Al and B<sub>4</sub>C. Spectroscopic analysis by SIMS (i.e., depth profiling) indicates that the nitrogen concentration varies linearly as a function of cryomilling time. A correlation between cryomilling time, nitrogen concentration, NC-Al grain size, and composite hardness was observed.

## Experimental procedures

Four trimodal Al MMCs with the same composition (50 wt% of CG-Al phase, 10 wt% of B<sub>4</sub>C powders, and 40 wt% of NC-Al phase), but cryomilled for different periods of time (8, 12, 16, and 24 h) have been examined in this study. A generalized manufacturing process for trimodal Al MMCs is illustrated in Fig. 1. Commercial gas-atomized AA5083 Al alloy powders and B<sub>4</sub>C particles were blended at a weight ratio of 4:1 and then cryomilled

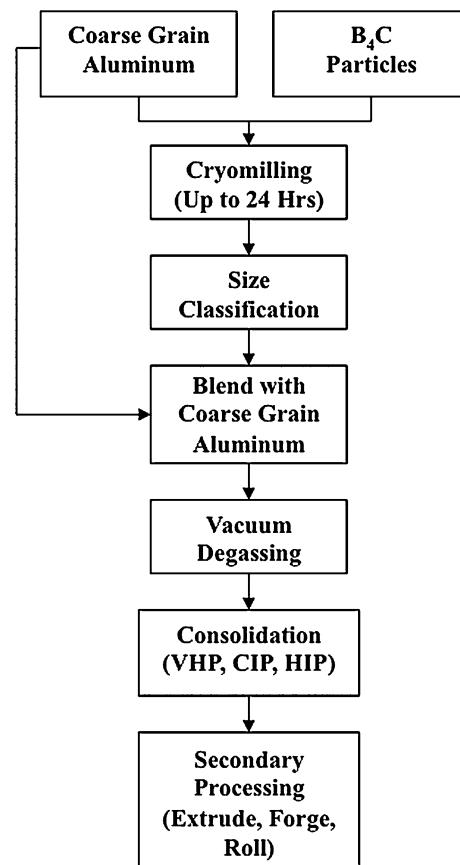


**Fig. 1** Typical manufacturing processing of trimodal Al MMCs

in liquid nitrogen. The AA5083 Al powders had an average particle size of less than 45 µm (Valimet Incorporated, Stockton, CA). The B<sub>4</sub>C particles (ESK Ceramics, Saline, MI) had a particle size ranging from 1 to 7 µm. A 1S Szegvari attritor, with a batch size of 1 kg of blended powders, was used for cryomilling. Stainless steel (440C) milling balls (1/4" diameter) were used with a ball-to-powder weight ratio of 32:1. The powders along with the milling balls were submerged in liquid nitrogen and milled with a rotation speed of 185 rpm. An addition of 0.2 wt% stearic acid (~50/50 palmitic and stearic acid) was used to improve the yield and minimize agglomeration. The cryomilled-powder slurry was then transferred into a glove box where the liquid nitrogen was allowed to evaporate, in order to minimize the contamination of the cryomilled-powders. The cryomilling process yields agglomerates of NC-Al grains containing a uniform dispersion of solidly bonded sub-micron B<sub>4</sub>C particles. The cryomilled-composite agglomerates were then homogeneously blended with unmilled-coarse grain AA5083 powders at an appropriate ratio. Thus, the fabricated composite consists of 10 wt% B<sub>4</sub>C, 50 wt% NC-Al, and 40 wt% CG-Al phases. A Type 304 stainless steel container was filled with blended powders in preparation for vacuum degassing. The

powders were degassed by heating the container to 395 °C for 6 h under a vacuum. In this study, the vacuum-degassed powders were consolidated into billets by CIP at a pressure of 310 MPa, followed by high strain rate (HSR) extrusion with a reduction ratio of 6:1 at 524 °C.

The trimodal Al MMCs fabricated for this study were characterized by optical microscopy (OM), scanning electron microscopy (SEM), TEM, and SIMS. OM was used to investigate the hierarchical microstructure (e.g., the size and distribution of CG-Al domains and NC-Al/B<sub>4</sub>C agglomerates). SEM analysis was performed using a Zeiss Ultra-55 field emission SEM to study B<sub>4</sub>C particle size and distribution. The influence of the hierarchical microstructure and B<sub>4</sub>C particle size and distribution, along with other specimens examined, will be reported elsewhere. However, the four specimens reported in this paper had similar hierarchical microstructure and B<sub>4</sub>C particle size and distribution. Specimens for TEM were prepared with a focused ion beam (FIB) in situ lift-out (INLO) technique using a FEI TEM-200. The FEI/Tecnai F30 300 keV TEM/STEM microscope was used for the TEM analysis. A variety of TEM techniques have been utilized including EELS, HRTEM, X-ray energy dispersive spectroscopy (XEDS), and HCDF. The HCDF-TEM imaging is a useful technique which provides

a much higher grain-to-grain contrast for most, if not all grains in the field of view compared to conventional bright field (BF) or dark field (DF) images. The HCDF-TEM enables a more efficient and statistically confident quantification of grain size and grain size distribution of the NC-Al phase. A detailed description of this technique can be found elsewhere [15]. The CAMECA IMS3F SIMS was used to quantify the composition and contamination in each sample. Using the depth profile technique with Al as the matrix, the elements examined include Al2, 14N, 12C, 10B + 11B, H, Al/2, Mg/2 and Mn. The Al2, a double pair of Al ions, was chosen over the single ion Al due to the interest in keeping all the elements within the same filter (electron multiplier) for purposes of consistency. All counts were normalized to an Al2 count that served as an internal standard. Hardness was measured by using the MacroMet 5100 series Rockwell Hardness tester on the B scale with a 100 kg load and a 1/16 brail indenter.

## Results and discussion

A typical multi-scale microstructure of the trimodal Al MMCs examined in this study is presented in Fig. 2.

**Fig. 2** Microstructure of trimodal Al MMCs: **a** typical optical micrograph normal to the extrusion, and **b** in the extrusion direction; **c** BF-TEM micrograph of trimodal microstructural features; **d** HCDF micrograph showing the nano grain size of NC-Al phase. These micrographs were obtained from trimodal Al MMCs produced with CG-Al powders and B<sub>4</sub>C/NC-Al agglomerates that were cryomilled for 8 h

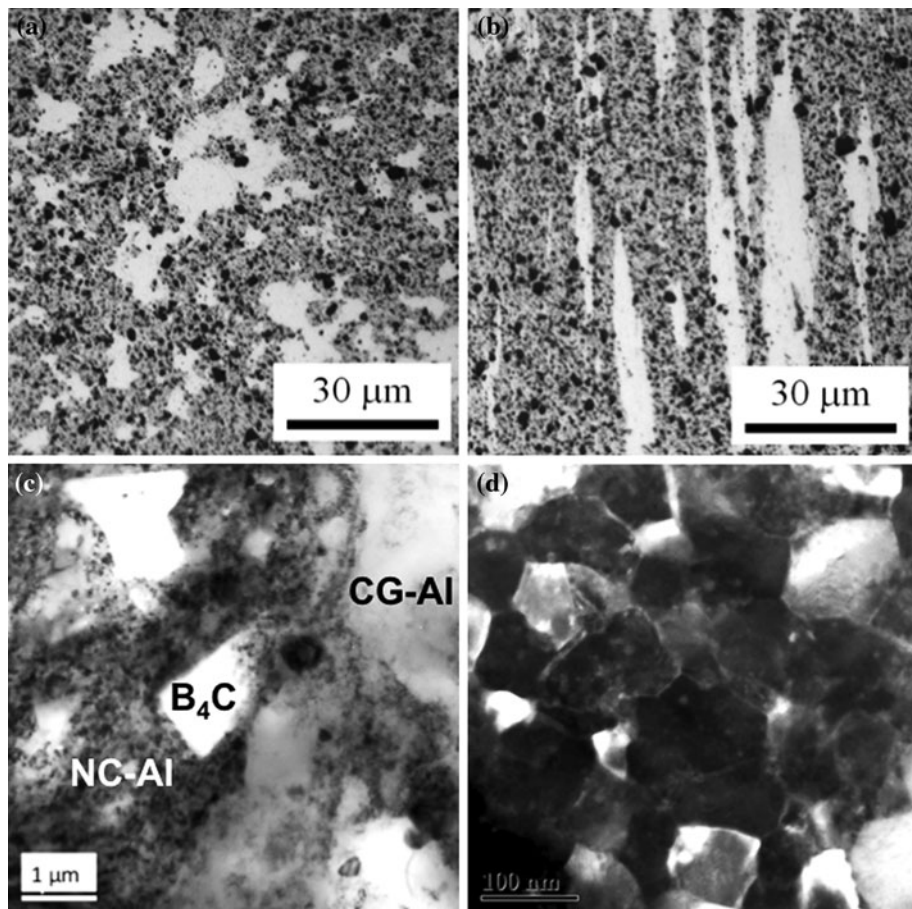
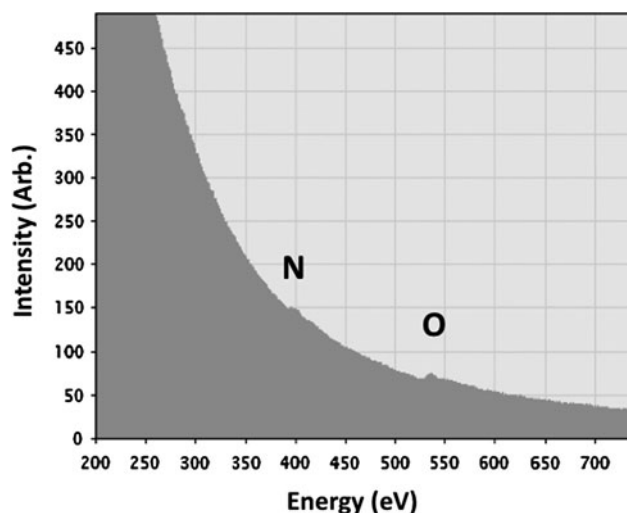


Figure 2a, b shows the optical micrographs normal to the extrusion direction and in the extrusion direction, respectively. The CG-Al domains appear as bright regions, while the B<sub>4</sub>C reinforced NC-Al domains appear as dark regions. Figure 2b further illustrates the elongated CG-Al structure as a result of the HSR extrusion deformation process. Figure 2c shows a BF-TEM micrograph that illustrates the multi-scale microstructure of the composites that includes NC-Al, B<sub>4</sub>C particles, and CG-Al. Figure 2d presents the HCDF-TEM micrographs of NC-Al phase. These features of Al-based trimodal MMCs are consistent with previously reported microstructures [7–9, 16].

The TEM examination of nitrogen distribution and structure within the composite is not trivial [14, 17]. In our study, the EELS technique under HRTEM mode was applied to detect nitrogen, and the electron beam was focused for subsequent analysis. This approach possesses the following merits. Since nitrogen generally has a relatively low concentration and nitrogen-containing dispersoids are expected to have a very small size (typically less than 10 nm), a focused electron beam in HRTEM mode can decrease the total electron-sample interaction volume, allowing easier detection of nitrogen through the EELS spectrum. Furthermore, it is more convenient to extract the structural information through the HRTEM images once the nitrogen-containing sites are identified. Thus, the sample is simply moved around to search for nitrogen based on the appearance of nitrogen peak in the EELS spectrum. Other TEM techniques, such as element mapping (e.g., energy filtered TEM or XEDS), have also been used. However, they were not capable of detecting the nitrogen due to its low concentration within the composites.

A typical EELS spectrum obtained from a nitrogen-containing region is presented in Fig. 3. The low intensity of the nitrogen signal yield is due to a low concentration of aluminum nitride as compared to the total interaction volume of electron beam with the specimen. From hundreds of TEM sites examined by EELS only a few sites yielded a relatively high concentration of nitrogen.

To identify the constituent structure of nitrogen dispersoids present in the composites, HRTEM micrographs were taken at sites where nitrogen was observed by EELS. Typical HRTEM images from these regions are presented in Fig. 4. Nitrogen was present within the trimodal Al MMCs in various forms: amorphous domains within the NC-Al grains (Fig. 4a), amorphous interfaces between NC-Al and B<sub>4</sub>C (Fig. 4b), and crystalline AlN typically at NC-Al grain boundaries (Fig. 4c). The Fast Fourier Transformation of the amorphous domains within the NC-Al grains confirms the absence of the crystalline phase. It should be noted that in Fig. 4b, nitrogen was *not* detected by EELS in the neighboring B<sub>4</sub>C particles and NC-Al grains, but only at the interface. The EELS and HRTEM



**Fig. 3** A typical EELS showing the N presence within the trimodal Al MMCs produced with CG-Al powders and B<sub>4</sub>C/NC-Al agglomerates that were cryomilled for 24 h

examination of the amorphous domains and B<sub>4</sub>C/NC-Al interfaces demonstrate that nitrogen can exist within an amorphous domain also containing high concentrations of aluminum, nitrogen, and oxygen. The crystalline AlN observed (Fig. 4c) would be due to the crystallization of the metallic amorphous phase or a reaction of trapped nitrogen with aluminum during the high temperature vacuum degassing and consolidation process.

The presence of localized nitrogen-rich domains could be ascribed to the cryomilling process. When two grains (Al and Al, or Al and B<sub>4</sub>C) collide and *weld* with each other during cryomilling, nitrogen can be mechanically trapped between interfaces and mechanically alloyed with surrounding Al or B<sub>4</sub>C phases during the severe plastic deformation inherent to the cryomilling process. A supersaturation of nitrogen may destabilize the FCC crystalline phase of the Al under severe plastic deformation and lead to the formation of non-equilibrium amorphous phases. The presence of amorphous domains is expected to significantly influence the mechanical properties of trimodal Al MMCs, since amorphous phases are generally much stronger than their crystalline counterparts given the same composition [18, 19]. These amorphous domains and crystalline AlN within NC-Al grains can increase the composite strength by dispersion-strengthening mechanisms.

The overall nitrogen concentration, NC-Al grain size, and mechanical properties of the trimodal Al MMCs with a variation in cryomilling time were quantified and correlated. The normalized nitrogen (14N/Al2) spectra for the four samples examined in this study are shown in Fig. 5. As the depth of SIMS profiling increases, typically into a few micrometers, the nitrogen count stabilizes to a value that reflects the bulk nitrogen content. The stabilized count

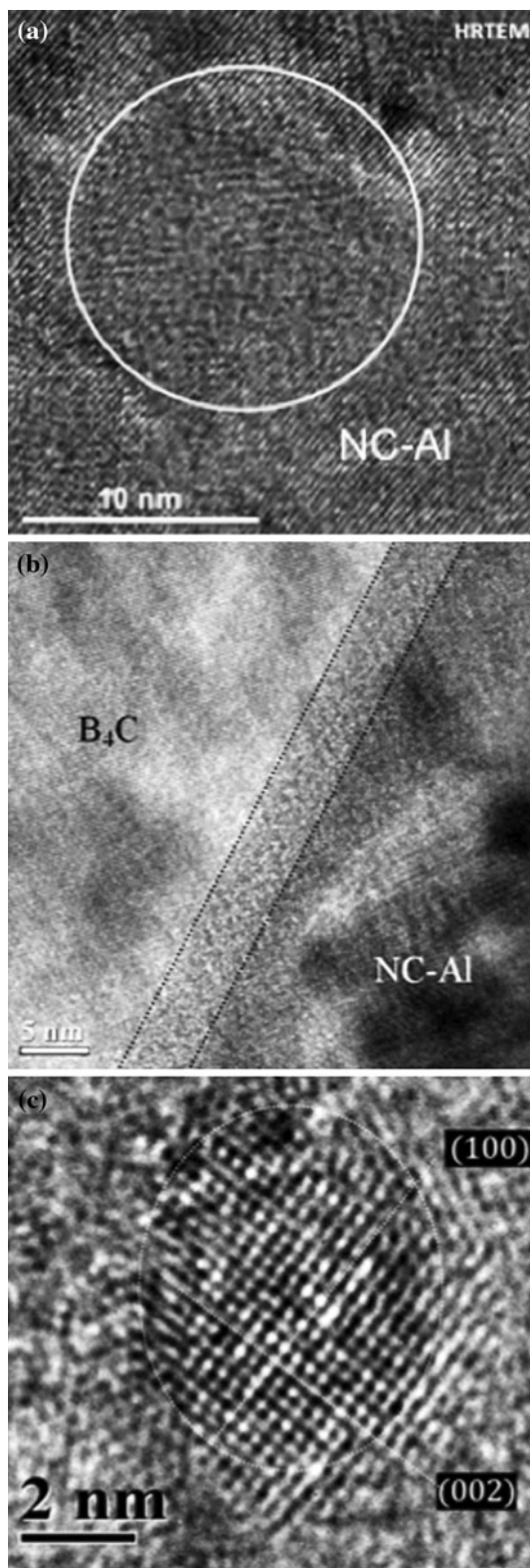


**Fig. 4** Various forms of nitrogen present within trimodal Al MMCs. **a** Amorphous domain in NC-Al grain. **b** Amorphous interface between NC-Al and  $B_4C$ . **c** Crystalline AlN. These micrographs were obtained from trimodal Al MMCs produced with CG-Al powders and  $B_4C/NC-Al$  agglomerates that were cryomilled for 24 h

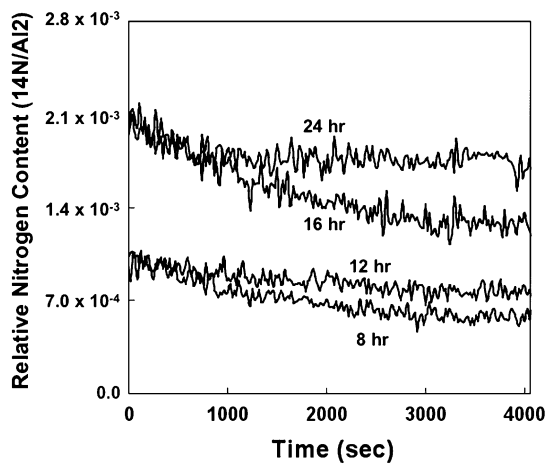


**Fig. 5** Typical SIMS depth profile results for measuring relative nitrogen content ( $14N/Al_2$ ) in trimodal Al MMCs

rate was employed to represent the nitrogen content within the trimodal Al MMCs. Figure 6 demonstrates that the normalized nitrogen content ( $14N/Al_2$ ) increases linearly as a function of cryomilling time up to 24 h. The standard deviation of nitrogen content, measured at least three times for each specimen, is negligible, i.e., smaller than the symbol used to represent the data in Fig. 6. An increase in nitrogen concentration with an increase in cryomilling time can be understood from the mechanical trapping postulation. Since nitrogen may be mechanically trapped at the interface between NC-Al and  $B_4C$ , as well as NC-Al and NC-Al during cryomilling, longer period of milling process would trap more nitrogen, and yield a higher nitrogen concentration. Saturation of nitrogen content was not observed even after 24 h of cryomilling.

Figure 7 presents the variation in NC-Al grain size and hardness as a function of nitrogen concentration. The cryomilling process reportedly reduces the NC-Al grain size rapidly so that the average grain size of powders after

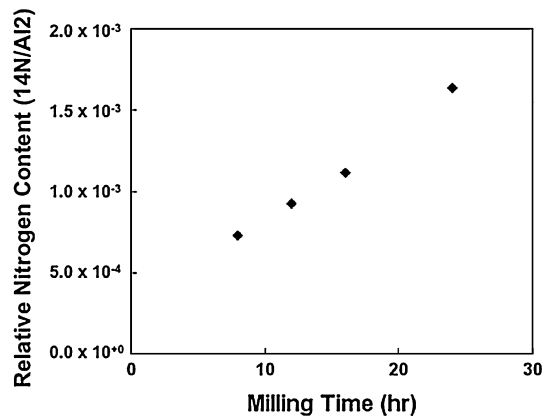


**Fig. 6** Relative nitrogen content ( $14N/Al_2$ ) measured for trimodal Al MMCs by SIMS as a function of cryomilling time

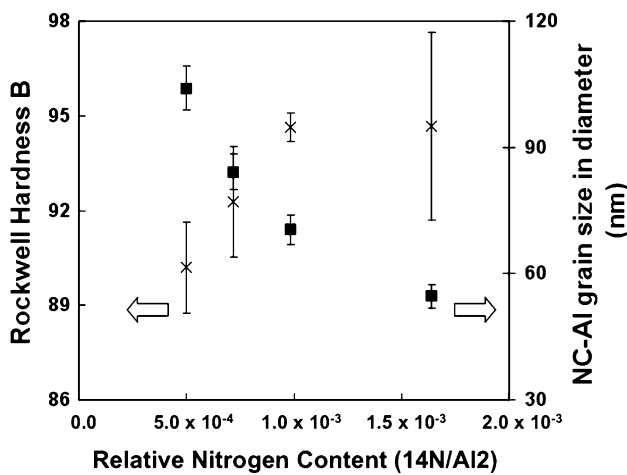


**Fig. 7** Rockwell hardness and grain size of NC-Al phase as a function of nitrogen content. The Rockwell Hardness is represented by symbol ‘x’ while the NC-Al grain size is represented by a solid square

4 h of milling is close to its minimum limiting value [11, 14]. It should follow that the specimens examined in this study have similar NC-Al grain size. The difference in NC-Al grain size in the composites would be due to the difference in *ability of nitrogen-containing dispersoids to inhibit* the growth of NC-Al grains during subsequent processing. In specimens with a high concentration of nitrogen, the various forms of nitride can significantly retard the NC-Al grain growth due to the pinning effect at or near the grain boundaries. Also seen in Fig. 7 is the correlation between the hardness and nitrogen content. An increase in composite hardness with an increase in nitrogen content is attributed to the reduction in NC-Al grain size and an increase in population of nitrogen-containing dispersoids. First, composites with a higher concentration of nitrogen possess a greater ability to inhibit NC-Al grain growth during high temperature processing, which has been clearly demonstrated. Furthermore, a higher concentration of amorphous and crystalline AlN dispersoids and, perhaps nitrogen in solid solution, induced by an increase in nitrogen concentration, would result in a stronger interaction with dislocations in the NC-Al phase, viz-a-viz, Orowan strengthening.

## Conclusions

The excellent thermal stability of NC-Al grains and the high strength of trimodal Al MMCs have been attributed to the presence of dispersoids containing nitrogen introduced during the cryomilling process. Analytical TEM and SIMS techniques have been applied to examine the structure of nitrogen-containing dispersoids and the total concentration of nitrogen, respectively. The nitrogen concentration varies

linearly with duration of cryomilling up to 24 h. Amorphous aluminum nitrides were typically observed within the NC-Al and at the NC-Al/B<sub>4</sub>C interface while crystalline nitrides were observed more frequently at the grain boundaries of NC-Al. Clear correlations among the total nitrogen concentration, NC-Al grain size, and composite hardness were observed. Exceptional mechanical properties of trimodal Al MMCs are attributed to the presence of nitrogen, in the form of strengthening dispersoids that also act as grain growth inhibitors.

**Acknowledgements** Research was sponsored by U.S. Army Research Laboratory and was accomplished under Cooperative Agreement W911NF-08-2-0026. The views, opinions, and conclusions made in this document are those of the authors and should not be interpreted as representing the official policies, either expressed or implied, of Army Research Laboratory or the U.S. Government. The U.S. Government is authorized to reproduce and distribute reprints for Government purposes notwithstanding any copyright notation herein.

## References

- Miracle DB, Donaldson SL (1999) Introduction to composites, volume 21 of ASM handbook. ASM International, Ohio, USA, p 39
- Eckert J, Calin M, Yu P, Zhang LC, Scudino S, Duhamel C (2008) Rev Adv Mater Sci 18(2):169
- Battezzati L, Pozzovivo S, Rizzi P (2004) Encycl Nanosci Nanotechnol 6:341
- Ma E (2003) Scripta Mater 49(7):663
- Koch CC, Morris DG, Lu K, Inoue A (1999) Mater Res Soc Bull 24(2):54
- Lergos M, Elliott BR, Rittner MN, Weertman JR, Hemker KJ (2000) Philos Mag A 80(4):1017
- Ye J, Han BQ, Lee Z, Ahn B, Nutt SR, Schoenung JM (2005) Scripta Mater 53(5):481
- Ye J, Han BQ, Lee Z, Ahn B, Nutt SR, Schoenung JM (6–11 February 2005) In: Trends in materials and manufacturing technologies for transportation industries and powder metallurgy research and development in the transportation industry, MPMD Global innovations proceedings held at the TMS Annual Meeting. San Francisco, CA, USA, p 383
- Ye J, Han BQ, Tang F, Schoenung JM (2005) In: Materials research society symposium proceedings 880E (mechanical properties of nanostructured materials): Paper #: BB1.5
- Lavernia EJ, Han BQ, Schoenung JM (2008) Mater Sci Eng A A493(1–2):207
- Ye J, Lee Z, Ahn B, He J, Nutt SR, Schoenung JM (2006) Metall Mater Trans A 37A(10):3111
- Van D, Thomas J, Bampton CC (2008) US Pat Appl Publ 10388059, 16 pp
- Van Daam, Thomas J, Bampton CC (2004) US Pat Appl US 2004177723 A1 20040916, 10 pp
- Witkin DB, Lavernia EJ (2006) Prog Mater Sci 51(1):1
- Yao B, Sun T, Warren A, Heinrich H, Barmak K, Coffey KR (2010) Micron 41:177
- Vogt RG, Zhang Z, Topping TD, Lavernia EJ, Schoenung JM (2009) J Mater Process Technol 11:5046
- Li Y, Liu W, Ortalan V, Li WF, Zhang Z, Vogt R, Browning ND, Lavernia EJ, Schoenung JM (2010) Acta Mater 58:1732
- Greer AL, Ma E (2007) MRS Bull 32(8):611
- Masumoto T (2001) Materia 40(11):925